PERKIN 2

Structure, conformation, anomeric effects and rotational barriers in the HERON amides, *N*,*N′*-diacyl-*N*,*N′*-dialkoxyhydrazines

Stephen A. Glover,*[a] Guoning Mo,[a] Arvi Rauk,[b] David J. Tucker[a] and Peter Turner[c]

[a] *Division of Chemistry, School of Physical Sciences, University of New England, Armidale 2351, New South Wales, Australia*
[b] *Department of Chemistry, University of Calgary, Calgary, AB, Canada T2N 1N4*
[c] *School of Chemistry, University of Sydney, Sydney 2006, New South Wales, Australia*

Received (in Cambridge, UK) 8th June 1999, Accepted 10th August 1999

N,*N′*-Diacyl-*N*,*N′*-dialkoxyhydrazines are HERON amides that exhibit theoretical and physical properties of bisheteroatom-substituted amides. Amide nitrogens are pyramidal and they adopt a preferential conformation which permits an anomeric interaction in which one nitrogen overlaps strongly with the adjacent N–O σ* orbital. A crystal structure of *N*,*N′*-di(*p*-chlorobenzoyl)-*N*,*N′*-diethoxyhydrazine **4d** has been obtained which confirms these properties in the solid state. Infrared data for ten such hydrazines indicate unusually high carbonyl stretch frequencies in accord with pyramidality at nitrogen. Diastereotopic resonances and dynamic ^{1}H NMR studies indicate both a significant N–N rotational barrier of between 65 and 72 kJ mol^{-1}, which is consistent with a strong anomeric interaction, as well as a much smaller than usual amide rotation barrier of 54 kJ mol^{-1}, a direct consequence of pyramidality at nitrogen.

Introduction

Amides which are geminally substituted with two electronegative heteroatoms at nitrogen have quite different physical and chemical properties when compared to primary amides, *N*-alkylamides or those with only one heteroatom such as hydroxamic esters.[1] The effect of the combined electronegativity of the substituents is to favour sp^3 hybridisation at the amide nitrogen since this puts maximum electron density close to the electronegative atoms. The net geometry at nitrogen is however the result of this effect and the normal tendency of the nitrogen lone pair to delocalise onto the more electronegative carbonyl oxygen, a process that is optimised by sp^2 hybridisation at nitrogen [Fig. 1(a)]. Deviation from the normal sp^2 hybridisation at nitrogen should therefore result in decreased amide resonance with a number of important consequences: shorter amide carbonyl bonds and higher carbonyl stretch frequencies in the infrared; longer N–C bonds and reduced *E*/*Z* isomerisation barriers. In addition, when the amide nitrogen becomes pyramidal, the non-bonded electron pair(s) of one heteroatom may donate effectively into the low-lying antibonding orbital of the other heteroatom's bond to the nitrogen and *vice versa* [Fig. 1(b)]. The latter interactions, also called negative hyperconjugation, we refer to collectively as anomeric effects and they should lead to predictable and observable structural changes. While either heteroatom can be a donor, the anomeric effect involving donation of the highest energy lone pair, say that of Y, into the lowest energy σ* orbital (in this case σ^*_{NX}) will predominate. This would lead to the following structural changes: a shortening of the N–Y bond and a significant increase in the rotational barrier about this bond as a consequence of pi overlap; longer N–X bonds as a consequence of increased occupation of the N–X antibonding orbital and therefore a reduced N–X rotational barrier. In fact, operation in one direction will tend to disfavour the reverse anomeric effect for two reasons; firstly the longer N–X bond disfavours pi donation from a lone pair on X and secondly, the shorter N–Y bond raises the energy of the N–Y antibonding orbital. Where the anomeric interaction is sufficiently strong, elimination or rearrangement of X becomes a chemical possibility. Inversion at nitrogen is predicted to be a low energy process since, in the planar transition state, nitrogen is sp^2 hybridised and the lone pair can conjugate fully with the carbonyl [Fig. 1(c)].

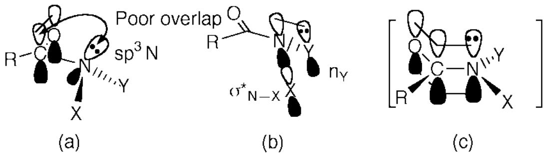

Fig. 1 (a) Pyramidal nitrogen; (b) anomeric interaction; (c) nitrogen inversion transition state in a bisheteroatom-substituted amide.

We have explored, theoretically, the structural characteristics of this class of amides and confirmed the operation of such effects[2] and in a comprehensive review, we recently focused on the relative anomeric effects, theoretical, spectroscopic and chemical properties of a number of different classes of bisheteroatom-substituted amides including *N*,*N*-dialkoxyamides (ONO systems), *N*-acyloxy-*N*-alkoxyamides (AcONO systems), *N*-alkoxy-*N*-haloamides (ONX systems) and *N*-alkoxy-*N*-aminoamides (NNO systems).[1] The *N*-alkoxy-(*N*-methylanilino)benzamide **1**, an example of a NNO system, was first encountered in the reaction of mutagenic *N*-acetoxy-*N*-alkoxybenzamides and *N*-methylaniline (Scheme 1).[3,4] In methanol, S$_N$2 reaction at the amide nitrogen and displacement

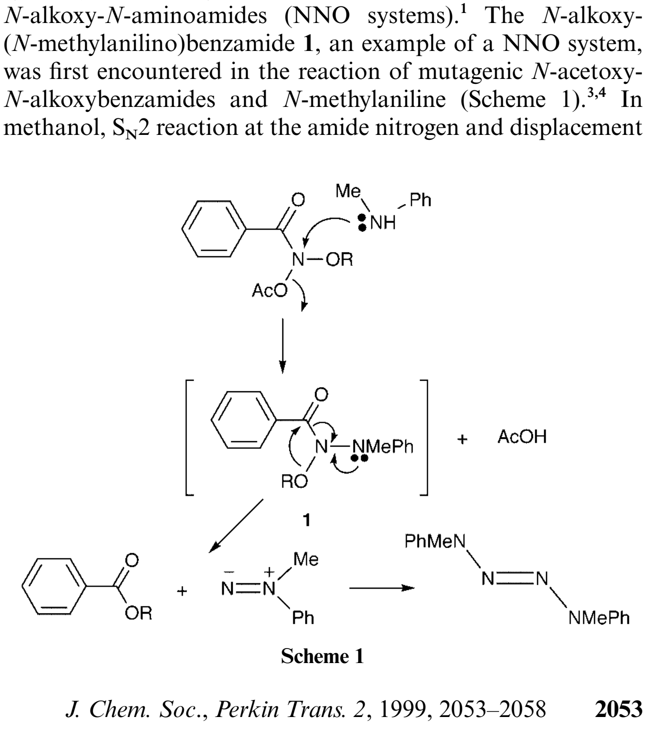

Scheme 1

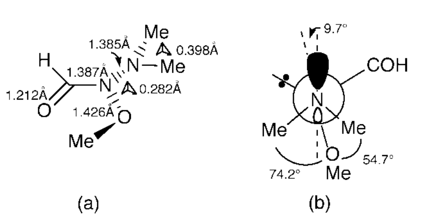

Fig. 2 (a) B3LYP/6-31G(d) optimised configuration for *N*-(dimethylamino)-*N*-methoxyformamide (**3**); (b) Newman projection along the N–N bond.

of acetate results in the formation of **1** as an unstable intermediate which undergoes a concerted migration of the alkoxy group to form benzoate esters and a 1,1-diazene. We have called these novel reactions, involving *HE*teroatom *R*earrangements *O*n *N*itrogen, HERON rearrangements and the amides so predisposed, HERON amides.[5]

N,*N*′-Diacyl-*N*,*N*′-dialkoxyhydrazines **2** are a class of thermally labile hydrazines that can be formed by dimerisation of alkoxyamidyl radicals formed either through oxidation of the parent hydroxamic esters[6–9] or through photolysis of *N*-halo-*N*-alkoxyamides.[10] They constitute anomeric amides in which the donor amino group is substituted with both an alkoxy and an acyl group and they are sufficiently stable to be isolated at room temperature. However, it is well established that they undergo thermal decomposition to give esters and nitrogen in a concerted process which we[11] and others[7] recently showed to involve consecutive HERON reactions (Scheme 2).

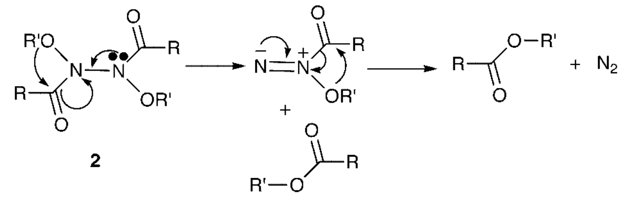

Scheme 2

Using semiempirical AM1 calculations, both we and Barton and coworkers predicted the first HERON step to be rate determining and the second HERON process of the 1-acyl-1-alkoxydiazene to be extremely fast.

The energetics and properties of the HERON reaction of the model *N*-methoxy-*N*-dimethylaminoformamide (**3**) have been thoroughly explored at the B3LYP/6-31G(D) level and the theoretical properties have been confirmed by kinetic investigations and studies of substituent effects in **2**.[12]

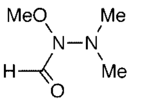

3

In the NNO systems, anomeric overlap is facilitated by the electronegativity of oxygen, the similarity in sizes of the interacting orbitals and, most importantly, the high energy lone pair on nitrogen. In the context of anomeric interactions the nitrogen lone pair is the highest in energy along the second row and should interact strongly with σ^*_{NO} orbitals in these systems. In a recent computational paper we have reported details of the stereoisomerism in the model *N*-methoxy-*N*-(dimethylamino)-formamide (**3**).[13] In summary, for the global minimum the amide nitrogen deviates significantly from planarity [Fig. 2(a)] which results in an *E*/*Z* amide rotational barrier of 53 kJ mol^{-1}, significantly smaller than that found in amides or hydroxamic esters (70–90 kJ mol^{-1}). Accordingly the carbonyl stretch frequency should be higher than in normal amides.[1] In addition, the favourable n_N–σ^*_{NO} orbital overlap [Fig. 2(b)] results in a long N–O bond and a short N–N bond with a significant barrier to rotation of 60 kJ mol^{-1}. As with all anomeric amides studied to date,[2] inversion at the amide nitrogen is computed to have a very low barrier on account of the planar, sp^2 hybridised nitrogen in the transition state [*cf*. Fig. 1(c)].

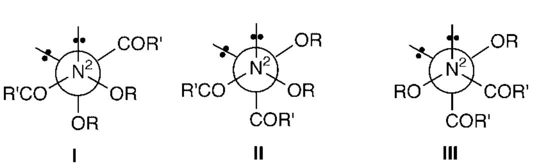

Fig. 3 Newman projections (N^2 to N^1) of staggered conformations of *N*,*N*′-diacyl-*N*,*N*′-dialkoxyhydrazines with lone pairs *syn*.

The *N*,*N*′-diacyl-*N*,*N*′-dialkoxyhydrazines **2** are a special case of the HERON amide **3** and in this paper, the theoretical, physical and spectroscopic properties of these hydrazines are discussed in detail.

Results and discussion

In hydrazines **2**, the n_N lone pair should be lowered in energy as a consequence of substitution by electron-withdrawing alkoxy and acyl groups. As a consequence, a weaker anomeric interaction is predicted. This is borne out by the higher theoretical and experimental activation energies for the anomerically driven HERON rearrangement of **2**[5,12] relative to **1** which cannot be isolated and rearrange rapidly at room temperature. Furthermore activation energies for the rearrangement of **4** increase in the order **4a** to **4e**.[12] Nonetheless, these hydrazines should, to a large extent, exhibit spectral characteristics and isomerisation barriers similar to those predicted for the model *N*-methoxy-*N*-(dimethylamino)formamide (**3**).

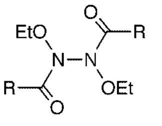

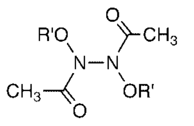

4

a: R = *p*-CH$_3$OC$_6$H$_4$
b: R = *p*-CH$_3$C$_6$H$_4$
c: R = C$_6$H$_4$
d: R = *p*-ClC$_6$H$_4$
e: R = *p*-NO$_2$C$_6$H$_4$

5

a: R′ = *p*-CH$_3$OC$_6$H$_4$CH$_2$
b: R′ = *p*-CH$_3$C$_6$H$_4$CH$_2$
c: R′ = C$_6$H$_4$CH$_2$
d: R′ = *p*-ClC$_6$H$_4$CH$_2$
e: R′ = *p*-NO$_2$C$_6$H$_4$CH$_2$

Structurally, if both nitrogens are pyramidal, as predicted for bisheteroatom-substituted amides, these hydrazines can exist in two conformations about the N–N bond that permit an anomeric overlap (Fig. 3, **I** and **II**). A mutual anomeric interaction is possible in conformation **I**, while in **II**, only one anomeric interaction is possible. The second interaction in **II** is minimal on account of the *syn gauche* relationship between the N^2 lone pair and the vicinal N^1–O bond. In these systems, the amide groups can also have both *E* and *Z* configurations. Thus conformational analysis yields one anti-symmetrical (*EZ*) and two symmetrical starting conformations (*EE* and *ZZ*) for **I** and four anti-symmetrical (*EE*, *ZZ*, *EZ* and *ZE*) starting conformations for **II**.†

RHF/6-31G* *ab initio* calculations on these fully relaxed conformations of the model *N*,*N*′-diformyl-*N*,*N*′-dimethoxyhydrazine (**I**–**III**, R′ = H, R = Me) predict that they have very similar energies, **II** *EE* being the most stable although **II** *ZE*, **I** *EE* and **I** *EZ* are very similar in energy (Table 1). **I** *EE* and **I** *ZZ* resulted in symmetrical structures. Conformer **III**, in which both anomeric interactions are minimised, appears not to be a stationary point on the energy surface and geometry optimisation resulted in one of the more stable, anomeric structures.

---

† The first stereochemical designator refers to the amide conformation at N^2 and the second refers to the conformation at N^1.

Table 1 Relative energies, bond lengths and pyramidal character at nitrogen for RHF/6-31G* optimised conformations of *N*,*N*′-diformyl-*N*,*N*′-dimethoxyhydrazine together with data for X-ray structure of **4d** as well as the RHF/6-31G*-optimised structure of **3**

Structure energy/ kJ mol$^{-1\,c}$	N–N/Å	N^1–C/Å	N^{1}C=O/Å	N^1–O/Å	N^2–C/Å	N^{2}C=O/Å	N^2–O/Å	ΔN^1/Å^a (angle/°)^d	ΔN^2/Å^b (angle/°)^d
I *EE* (+1.1)	1.354	1.387	1.183	1.374				0.313(114.9)	
I *EZ* (+2.7)	1.356	1.380	1.183	1.363	1.399	1.180	1.379	0.274(116.1)	0.352(113.7)
I *ZZ* (+4.5)	1.361	1.394	1.180	1.372				0.344(114.0)	
II *ZE* (+0.9)	1.361	1.398	1.180	1.371	1.390	1.180	1.366	0.339(114.1)	0.311(115.0)
II *EE* (0.0)	1.355	1.387	1.182	1.367	1.393	1.181	1.373	0.289(115.7)	0.315(114.9)
II *ZZ* (+5.2)	1.356	1.401	1.178	1.369	1.378	1.183	1.362	0.345(113.9)	0.235(117.1)
II *EZ* (+4.6)	1.352	1.388	1.181	1.363	1.383	1.183	1.371	0.288(115.7)	0.254(116.6)
3	1.379	1.378	1.087	1.375				0.321(115.0)	0.394(112.7)
4d	1.389(3)	1.412(3)	1.213(2)	1.403(2)	1.410(3)	1.207(3)	1.411(3)	0.334(114.4)	0.358(113.7)

[a] Deviation of N^1 from N^{2}CO plane. [b] Deviation of N^2 from N^{1}CO plane. [c] Relative to **II** *EE*. [d] Average angle at nitrogen.

Table 2 Infrared carbonyl absorption frequencies (cm^{-1}) for *N*,*N*′-diacyl-*N*,*N*′-dialkoxyhydrazines (R^{2}CON(OR^1)N(OR^1)COR^2) and precursor hydroxamic esters

R^1	R^2	Hydrazine (CHCl$_3$)	Hydrazine (Condensed phase)	Hydroxamic ester (CHCl$_3$)	Source
Et	*p*-$CH_3OC_6H_4$	1700	1717/1708 (nujol)	1681	[a]
Et	*p*-$CH_3C_6H_4$	1701	1712/1676 (nujol)	1682	[a]
Et	C_6H_5	1708	1696 (nujol)	1685	[a]
Et	*p*-ClC_6H_4	1711	1718/1679 (nujol)	1680	[a]
Et	*p*-$NO_2C_6H_4$	1722	1720/1695 (nujol)	1692	[a]
p-$CH_3OC_6H_4CH_2$	CH_3	1733/1707		1693	[a]
p-$CH_3C_6H_4CH_2$	CH_3	1734/1700		1693	[a]
$PhCH_2$	CH_3	1735/1711		1682	[a]
p-$ClC_6H_4CH_2$	CH_3	1738/1715		1693	[a]
p-$NO_2C_6H_4CH_2$	CH_3	1744/1723	1731 (nujol)	1700	[a]
CH_3	Ph		1718 (neat)	—	7
Bu^t	Ph		1685 (KBr)	—	7
Bu^t	1-adamantyl		1708 (neat)	1644 (neat)	7
CH_3	Bu^t		1684 (neat)	—	7
CH_3	$PhCH_2CH_2$		1725 (neat)	1685	7
$PhCH_2$	$PhCH_2CH_2$		1724 (neat)	—	7
CH_3	Cyclohexyl		1711 (KBr)	—	7

[a] This work.

In all cases, nitrogens were predicted to be pyramidal. The deviation from planarity (Table 1) correlates with increased N–O and N–CO bonds in each of the asymmetrical structures (**I** *EZ* and **II**). In general the more pyramidal of the two nitrogens within each conformer has longer bonds as a result of increased sp^3 character at that centre. N–O bond lengths are however controlled by at least two electronic effects; pyramidalisation at the nitrogen and anomeric donation from the adjacent nitrogen lone pair into the neighbouring σ^*_{NO} orbital. These are difficult to separate. However, since in two of the four cases where an anomeric effect is likely to be stronger in one direction (**II** *ZE, ZZ*) the N–O bond of the oxygen atom bonded to the more pyramidal, donor nitrogen is longer, the nature of hybridisation is likely to be the dominant effect. N–N bond lengths are similarly dependent upon pyramidalisation at nitrogens and anomeric effects. However, N–N bond lengths in series **I** and **II** do not differ significantly which suggests they have a similar degree of anomeric interaction. This must be largely in one direction in the case of **II**. Data for the asymmetric structure (**I** *EZ*) in fact also support the operation of an anomeric effect in one direction even though a mutual effect is possible. In this conformer, N^1, the donor atom, is significantly less pyramidal than N^2 and the N^2–O^2 bond is measurably longer than the N^1–O^1 bond. In this case, the pyramidalisation and anomeric effect work in the same direction. A comparison of the data for hydrazines **I** and **II** with those for the RHF/6-31G*-optimised geometry of **3** (Table 1) indicates that shorter N–N bonds prevail for the hydrazines. However, the dimethylamino nitrogen in **3** is strongly pyramidal (distance to plane 0.394 Å, average angle 112.7°) resulting in a longer N–N bond in spite of the stronger anomeric overlap that is possible in this system.

In two cases (**II** *ZZ* and **I** *EZ*) there is a marked difference in the degree of planarity at the nitrogens. In these cases at least, different carbonyl absorptions would be predicted in the infrared as carbonyls have significantly different equilibrium bond lengths.

Analysis of the infrared spectra for the two series of hydrazines **4** and **5** together with data reported by Barton and coworkers[7] indicates that the carbonyl stretch frequencies are all appreciably higher than the monoheteroatom-substituted precursor hydroxamic esters which is in accord with a significant degree of non-planarity at nitrogen (Table 2). In series **4**, as well as series **5**, the carbonyl absorptions generally increase in wavenumber as the aryl substituent is varied from electron donor to electron acceptor. The carbonyl stretch frequencies are a sensitive monitor of the electron demand at amide nitrogen. In addition, infrared spectroscopy also supports the unsymmetrical nature of some of these hydrazines. While the benzoyl series **4** appears to have degenerate or nearly degenerate carbonyl stretch frequencies in solution, in the solid state all but **4c** show two distinct carbonyl absorptions. In the benzyloxy series, **5**, two carbonyl absorptions are clearly evident in solution. Both are affected in a predictable fashion by electronic effects of the substituents.

A low temperature X-ray structure of *N*,*N*′-di(*p*-chlorobenzoyl)-*N*,*N*′-diethoxyhydrazine **4d** confirms the unsymmetrical nature of this substrate. The conformation in the solid-state is **II** *ZE* and, as predicted on both qualitative and

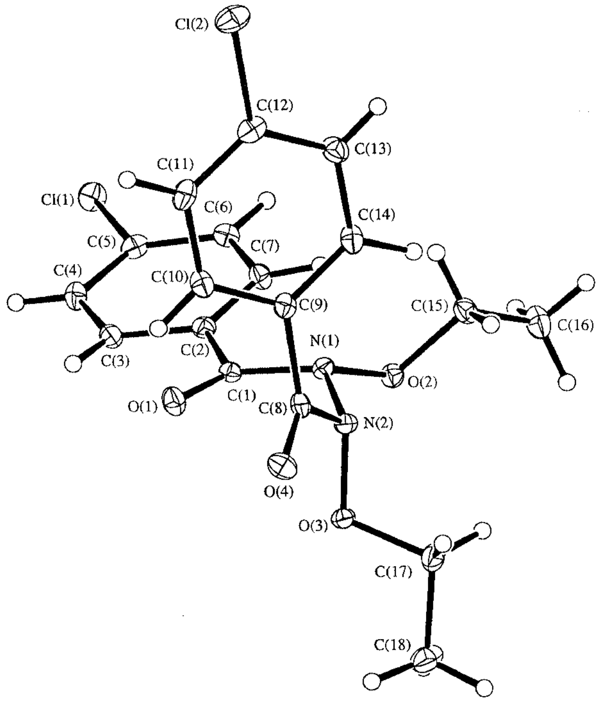

Fig. 4 ORTEP drawing of the crystal structure of *N*,*N*′-di(*p*-chlorobenzoyl)-*N*,*N*′-diethoxyhydrazine **4d** with thermal ellipsoids depicted at the 25% level.

theoretical grounds, both nitrogens are strongly pyramidal, making distances of 0.334 Å (N^1) and 0.358 Å (N^2) from the plane of the attached atoms (Fig. 4). The ethyl groups are both *exo* to the pyramidal nitrogens. This is the first structural confirmation of the effect of bisheteroatom-substitution upon amide nitrogens. The X-ray structure also shows evidence for an anomeric interaction in the direction of N^2. The N^2–O^3 bond nearly bisects the adjacent C^1–N^1–O^2 angle with torsion angles of 69.4(2)° and −66.7(2)° to N^1–C^1 and N^1–O^2 bonds respectively, while the N^2–O^3 bond is nearly 0.01 Å longer than the N^1–O^2 bond. Both could be accounted for by overlap between the N^1 lone pair and the N^2–O^3 antibonding orbital. This lone pair overlap would be expected to reduce further the conjugative overlap with the amide carbonyl attached to N^1 resulting in a shorter N^{1}C=O bond relative to N^{2}C=O. However, analysis shows that the *p*-chlorophenyl ring on the N^1 side of the molecule is nearly coplanar with the adjacent carbonyl (twist angle of 8°‡). The other aryl ring is tilted at an angle of 45°§ relative to the carbonyl attached to N^2. Contacts of both rings with adjacent molecules would appear to be minimal and, with regard to the *p*-chlorophenyl ring on the N^1 side, would, if anything, be reduced by a larger tilt angle. Near coplanarity in this case could be compensating to a degree for the weak conjugation into the carbonyl by the N^1 lone pair which is diverted toward the anomeric interaction. The carbonyl bond lengths are consequently similar although the N^{1}C=O carbonyl [1.213(2) Å] is marginally longer than the N^{2}C=O carbonyl [1.207(3) Å]. The origin of the radically different carbonyl infrared absorptions in the solid state ($\Delta\nu = 29$ cm^{-1}) was determined from a frequency calculation on the model conformer **II** *ZE*. RHF/6-31G* calculations of the normal modes of vibration predict, after scaling by a factor of 0.8737,[14,15] two strongly coupled carbonyl frequencies at 1786 cm^{-1} and 1768 cm^{-1}. In this conformation the carbonyls are relatively close (3.08 Å between carbons) and the dipoles make an angle of only 40° with respect to one another. Computed frequencies correspond to the symmetric and anti-symmetrical stretch respectively. In the X-ray structure (Fig. 4) the carbonyls are even closer (2.96 Å between carbons) and subtend an angle of only 38.0°. It is therefore likely that the carbonyl resonances would likewise be coupled and the infrared spectrum of **4d** in the condensed phase is consistent with this. The higher carbonyl absorption at 1718 cm^{-1} most likely corresponds to the symmetrically coupled vibrational mode and, in keeping with this, is more intense than the lower, anti-symmetrical frequency at 1679 cm^{-1}. In this respect, spectra for these diacylhydrazines parallel those found for anhydrides and diacylperoxides in which *cis* carbonyls are also found to be strongly coupled and the symmetrical stretch is both higher in frequency and also more intense than the anti-symmetrical mode.[16,17] RHF/6-31G* calculations on planar and twisted benzamide (carbonyl at 46° relative to the aryl ring) predict an increase of 0.023 Å in the C=O bond length of the planar form and a reduction in the carbonyl stretch frequency by about 18 cm^{-1}. Thus, in the solid state, the N^1 carbonyl should be lengthened and moved down in frequency towards that for the N^2 carbonyl by a similar amount leading to a strengthening of the vibrational coupling between the two.[17] In solution the bands are not resolved resulting in a broad carbonyl at 1711 cm^{-1}.

Interestingly, RHF/6-31G* calculations on the unsymmetrical model **I** *EZ* gives scaled frequencies at 1765 and 1781 cm^{-1} corresponding to stretch modes that are uncoupled and are largely associated with different carbonyls. The lower stretch frequency corresponds to the carbonyl attached to the (donor) more planar nitrogen which has a shorter N–CO bond. The carbonyls in this substrate are somewhat further apart and their dipoles subtend a much larger angle of 64°.

The ^{1}H NMR spectra of **4** and **5** displayed respectively an ABX$_3$ and an AB spin system for the oxymethylenic protons which are clearly diastereotopic. The barrier to nitrogen inversion is likely to be similar to that calculated for **3**[13] and other anomeric amides[1] and it is extremely unlikely that the inversion barrier is unattainable at room temperature. Nitrogen inversion is therefore expected to be rapid on the NMR timescale. Diastereotopism is thus most likely a consequence of restricted rotation about the N–N bond. Methylene protons in simple bipyramidal hydrazines topomerise through inversion–rotation processes avoiding high energy eclipsing of lone pairs. Free energy barriers to these isomerisations are in the region of only 42–46 kJ mol^{-1} and have been attributed to the rotation rather than the inversion process.[18] Here too, inversion processes are less demanding energetically.[19,20] N–N rotation barriers in pyramidal-planar and biplanar hydrazines are significantly higher (typically 67–71 and 84–96 kJ mol^{-1} respectively) because of the unavoidable involvement of lone pair–lone pair eclipsing in rotation processes.[18,19,21] Topomerisation of methylene protons in bipyramidal *N*,*N*′-diacyl-*N*,*N*′-dialkoxyhydrazines, **4** and **5** clearly involves a much higher energy barrier than that found for simple bipyramidal hydrazines since the methylene protons are resolved into tight AB systems well above room temperature. Conformational analysis shows that topomerisation can only be achieved by inversion at each nitrogen together with two rotations about the N–N bond. Conformer **IV** involves complete loss of anomeric interaction as does the second rotation, R(2) (Scheme 3). Since inversion processes are facile, an important contribution to the height of these barriers is the loss of anomeric overlap.

Fig. 5 illustrates coalescence, at high temperature, of the diastereotopic benzylic protons for *N*,*N*′-diacetyl-*N*,*N*′-di(*p*-chlorobenzyloxy)hydrazine **5d** in toluene-*d*$_8$. Topomerisation barriers, obtained from the coalescence temperatures of selected hydrazines, including **5d**, are given in Table 3 and can be regarded as a direct measure of the strength of anomeric overlap in these ONN systems; the transition state corresponds to a geometry in which each nitrogen lone pair is approximately

---

‡ Angle between plane {O^{1}C^{1}N^{1}C^2} and plane {C^{2}C^{3}C^{4}C^{5}C^{6}C^7} = 8.0(1)°.

§ Angle between plane {O^{4}C^{8}N^{2}C^9} and plane {C^{9}C^{10}C^{11}C^{12}C^{13}C^{14}} = 45.2(1)°.

Table 3 Dynamic ^1H NMR data and N–N rotation barriers for oxymethylenic protons of *N*,*N*′-diacyl-*N*,*N*′-dialkoxyhydrazines ($R^2CON(OR^1)$-$N(OR^1)COR^2$) **4** and **5**

	R^1	R^2	δ/ppm	$\Delta\nu$/Hz[a]	J_{AB}/Hz[a]	T_C/K	$\Delta G^{\ddagger}_{Tc}$/kJ mol^{-1}	Solvent
4a	Et	p-$CH_3OC_6H_4$	4.12	28.60	14.30	316	65.4	$CDCl_3$
4b	Et	p-$CH_3C_6H_4$	4.12	26.63	14.31	318	65.9	$CDCl_3$
4c	Et	C_6H_5	4.13	26.91	14.40	319	66.1	$CDCl_3$
4d	Et	p-ClC_6H_4	4.14	27.64	14.29	316	65.5	$CDCl_3$
4e	Et	p-$NO_2C_6H_4$	4.17	24.10	14.30	320	66.5	$CDCl_3$
5a	p-$CH_3OC_6H_4CH_2$	CH_3	4.98	8.21	10.79	338	71.6	toluene-d_8
5b	p-$CH_3C_6H_4CH_2$	CH_3	5.00	[b]	[b]	—	—	—
5c	$PhCH_2$	CH_3	5.04	7.24	18.46	336	69.7	toluene-d_8
5d	p-$ClC_6H_4CH_2$	CH_3	5.01	8.40	10.42	342	72.5	toluene-d_8
5f	p-$NO_2C_6H_4CH_2$	CH_3	5.20	17.37	11.55	346	72.8	toluene-d_8

[a] $\Delta\nu_{AB}$ and J_{AB} for benzylic methylene protons of **4a–e** were obtained by spectral simulation. [b] Benzylic methylene unresolved below coalescence.

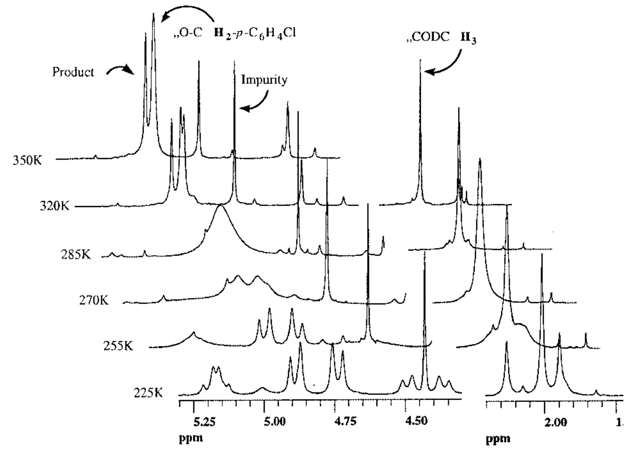

Fig. 5 Variable temperature ^1H NMR spectra of the benzylic methylene and acetyl methyl resonances of *N*,*N*′-diacetyl-*N*,*N*′-di(*p*-chlorobenzyloxy)hydrazine **5d** in toluene-d_8.

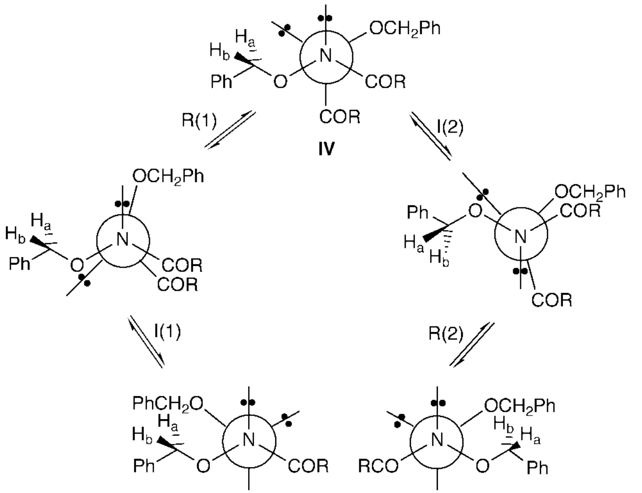

Scheme 3

orthogonal to the adjacent N–O bond and most probably resembles closely the central structure **IV** in Scheme 3.

In the case of *N*,*N*′-diacetyl-*N*,*N*′-di(*p*-chlorobenzyloxy)-hydrazine **5d** in toluene-d_8, the diastereotopic benzylic protons were significantly broadened at room temperature. Below 278 K they separated into three sets of diastereotopic methylenes (ratio 1 : 2 : 1) while the acetyl signal also resolved into three separate resonances in similar ratio (Fig. 5). Below 278 K, rotation about the amide N–C(O) bonds becomes slow on the NMR timescale and the spectrum probably indicates the presence of *gauche* conformations of a major, symmetrical form (**I** *EE* or **I** *ZZ*) centred on δ 4.8 and 2.0 and two different benzyl and acetyl resonances of an unsymmetrical form (**I** *EZ* or **II**) at δ 5.17, 4.42, 2.13 and 1.95. From the coalescence temperature, the barrier to amide rotation was estimated at $\Delta G^{\ddagger}_{278} = 54$ kJ mol^{-1} and accords with a significant reduction in amide conjugation in these systems. The barrier is similar to the theoretical one calculated for **3**,[13] but is greater than that determined experimentally for the *N*-acyloxaziridines **6**.[22] In these compounds the nitrogen is sp^3 hybridised and is constrained in a three-membered ring resulting in both high barriers to nitrogen inversion (46–50 kJ mol^{-1}) and very low barriers to rotation about the N–CO bond (42–43 kJ mol^{-1}). Accordingly, the carbonyl absorptions for **6** occur at 1740 cm^{-1} which is higher than those found for series **4** (Table 2).

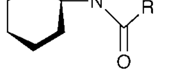

6

R = Me, Et, CH$_2$Ph

Conclusion

N,*N*′-Diacyl-*N*,*N*′-dialkoxyhydrazines exhibit all the characteristics of bisheteroatom-substituted amides. They have pyramidal nitrogens and sustain anomeric effects. Theoretical and structural evidence has been obtained for asymmetrical structures in which one nitrogen lone pair acts as donor to the neighbouring N–O σ* orbital. Solution infrared and NMR data are in accord with these properties since they exhibit high carbonyl stretch frequencies as well as low amide isomerisation barriers. In addition, the diastereotopism exhibited for methylenic protons in the room temperature ^1H NMR spectra indicates a significantly restricted rotation about the N–N bonds. This may be attributed to the operation of a negative hyperconjugative effect leading to partial pi bond character. As is the case for *N*-amino-*N*-alkoxyamides, the anomeric interaction is the driving force for HERON reaction of *N*,*N*′-diacyl-*N*,*N*′-dialkoxyhydrazines which leads to their thermal decomposition, at modest temperatures, to esters and nitrogen.

Experimental

The synthesis and characterisation of *N*,*N*′-diacyl-*N*,*N*′-dialkoxyhydrazines **4** and **5** have been detailed in a previous paper.[12]

Variable temperature NMR experiments

The variable temperature 300 MHz ^1H NMR experiments were carried out for *N*,*N*′-diacyl-*N*,*N*′-dialkoxyhydrazines (R^2CON-$(OR^1)N(OR^1)COR^2$) **4** and **5** on a Bruker AC-300P FT NMR spectrometer with BVT1000 variable-temperature accessory.

Table 4 Dynamic ^{1}H NMR data for methylene protons of **5d** in toluene-d_8 at low temperatures

	R^1	R^2	δ/ppm	$\Delta\nu$/Hz	J/Hz	T_C/K	$\Delta G^{\ddagger}_{Tc}$/kJ mol^{-1}	Solvent
5d	p-ClC$_6$H$_4$CH$_2$	CH$_3$	5.01	111.37	—	278	54	toluene-d_8

All samples were in either CDCl$_3$, with tetramethylsilane (0.1%) as an internal standard, or toluene-d_8, with methyl group (δ_H 2.3) of the trace isotope as a reference. The free energy of activation at the temperature of coalescence of an equally populated two-site system, $\Delta G^{\ddagger}$(kJ mol^{-1}), was calculated using a modified form (1) of the Eyring formulation.[23] A similar

$$\Delta G^{\ddagger} = 19.145 \times 10^{-3}/T_C[9.972 + \log(T_C/\Delta\nu)] \quad (1)$$

expression (2) can be derived for a coalescing AB system, $\Delta G^{\ddagger}$ (kJ mol^{-1}).

$$\Delta G^{\ddagger} = 19.145 \times 10^{-3}/T_C[9.972 + \log(T_C/\sqrt{(\Delta\nu^2 + 6J_{AB}^2)})] \quad (2)$$

The NMR data at high temperatures are given in Table 3 while those at low temperature for **5d** are presented in Table 4. For Series **4**, $\Delta\nu$ and J_{AB} below coalescence temperature were obtained using the PANIC spectral simulation program implemented on the ASPECT 3000 computer of the Bruker AC-300P FT NMR spectrometer. Spectra were simulated as an ABX$_3$ system.

X-Ray crystallography

Crystals of *N*,*N′*-di(*p*-chlorobenzoyl)-*N*,*N′*-diethoxyhydrazine **4d** were found to decompose in a diffractometer X-ray beam at room temperature, and accordingly a low temperature data collection was undertaken.¶ A colourless and approximately prismatic fragment cut from a large soft single crystal was attached to a glass fibre with Exxon Paratone N. The crystal was then quenched in a nitrogen cold stream at −80 °C on mounting on a Rigaku AFC7R diffractometer. An empirical absorption correction based on azimuthal scans of three reflections was applied and the data were also corrected for Lorentz and polarisation effects. Processing and calculations were undertaken with TEXSAN.[24] The structure was solved in the space group $P2_1/c$(#14) by direct methods with SIR92,[25] and extended and refined with SHELXL-97.[26] Anisotropic thermal parameters were refined for the 26 non-hydrogen atoms in the asymmetric unit of the structure model. The 18 hydrogen atoms were located and modelled with isotropic thermal parameters. An ORTEP[27] depiction of the molecule is provided in Fig. 4.

Details. Formula $C_{18}H_{18}Cl_2N_2O_4$, M 397.24, colourless, monoclinic, space group $P2_1/c$(#14), a 8.1227(5), b 10.1880(10), c 22.116(2) Å, β 91.450(6)°, V 1829.6(3) Å^3, D_c 1.442 g cm^{-3}, Z 4, crystal size 0.375 by 0.325 by 0.225 mm, λ(Cu-K$_\alpha$) 1.54178 Å, μ(Cu-K$_\alpha$) 3.426 cm^{-1}, T(psi)$_{min,max}$ 0.61, 0.99, θ_{max} 65.08, *hkl* range 0 9, 0 11, −23 25, N 3029, N_{ind} 2644(R_{merge} 0.091), N_{obs} 2470($I > 2\sigma(I)$), N_{var} 308, residuals|| $R1(F)$ 0.0567, $wR2(F^2)$ 0.1540, GoF(all) 1.053, $\Delta\rho_{min,max}$ −0.478, 0.543 e Å^{-3}.

Acknowledgements

The authors are grateful to the Australian Research Council and the Natural Sciences and Engineering Research Council of Canada for financial support and to the University of New England for a University of New England Research Grant and a U.N.E. Research Scholarship to G. M.

References

1 S. A. Glover, *Tetrahedron*, 1998, **54**, 7229; *Tetrahedron Report* 455.
2 S. A. Glover and A. Rauk, *J. Org. Chem.*, 1996, **61**, 2337.
3 J. J. Campbell and S. A. Glover, *J. Chem. Soc.*, *Perkin Trans. 2*, 1992, 1661.
4 J. J. Campbell and S. A. Glover, *J. Chem. Res. (S)*, 1999, **8**, 474.
5 J. M. Buccigross and S. A. Glover, *J. Chem. Soc.*, *Perkin Trans. 2*, 1995, 595.
6 J. H. Cooley, M. W. Mosher and M. A. Khan, *J. Am. Chem. Soc.*, 1968, **90**, 1867.
7 M. V. De Almeida, D. H. R. Barton, I. Bytheway, J. A. Ferreira, M. B. Hall, W. Liu, D. K. Taylor and L. Thomson, *J. Am. Chem. Soc.*, 1995, **117**, 4870.
8 A. R. Forrester, E. M. Johansson and R. H. Thomson, *J. Chem. Soc.*, *Perkin Trans. 1*, 1979, 1112.
9 R. O. C. Norman, R. Purchase and C. B. Thomas, *J. Chem. Soc.*, *Perkin Trans. 1*, 1972, 1701.
10 T. Koenig, J. A. Hoobler, C. E. Klopfenstein, G. Heddon, F. Sunderman and B. R. Russell, *J. Am. Chem. Soc.*, 1973, **96**, 4573.
11 J. M. Buccigross, S. A. Glover and G. P. Hammond, *Aust. J. Chem.*, 1995, **48**, 353.
12 S. A. Glover, G. Mo and A. Rauk, *Tetrahedron*, 1999, **55**, 3413.
13 S. Glover and A. Rauk, *J. Org. Chem.*, 1999, **64**, 2340.
14 J. A. Pople, A. P. Scott, M. W. Wong and L. Radom, *Isr. J. Chem.*, 1993, **33**, 345.
15 A. P. Scott and L. Radom, *J. Phys. Chem.*, 1996, **100**, 16502.
16 L. J. Bellamy, *The Infra-red Spectra of Complex Molecules*, Chapman and Hall, New York, 1975, 3rd Edn.
17 L. J. Bellamy, *Advances in Infrared Group Frequencies*, Methuan and Co. Ltd., Bungay, London, 1968.
18 J. R. Fletcher and I. O. Sutherland, *J. Chem. Soc.*, *Chem. Commun.*, 1969, 706.
19 Y. Shvo, in *The chemistry of the hydrazo, azo and azoxy groups Part 2*, ed. S. Patai, Wiley, London, 1975, pp. 1076–1080.
20 Y. Hamada, A. Y. Hirakawa, T. Tamagake and M. Tsuboi, *J. Mol. Spectrosc.*, 1970, **35**, 420.
21 G. J. Bishop, B. J. Price and I. O. Sutherland, *J. Chem. Soc.*, *Chem. Commun.*, 1967, 672.
22 W. B. Jennings, S. P. Watson and D. R. Boyd, *J. Chem. Soc.*, *Chem. Commun.*, 1992, 1078.
23 J. Sandström, *Dynamic NMR Spectroscopy*, Academic Press, London, 1982.
24 TEXSAN: Crystal Structure Analysis Package, Molecular Structure Corporation 1985 and 1992.
25 A. Altomare, M. Cascarano, C. Giacovazzo and A. Guagliardi, *J. Appl. Crystallogr.*, 1993, **26**, 343.
26 G. M. Sheldrick, SHELXL97, Program for Crystal Structure Refinement, University of Göttingen, Germany, 1997.
27 C. K. Johnson, ORTEPII, Report ORNL-5138, Oak Ridge National Laboratory, Oak Ridge, Tennessee, 1976.

Paper 9/04575I

¶ CCDC reference number 188/182. See http://www.rsc.org/suppdata/p2/1999/2053 for crystallographic files in .cif format.

|| $R1 = \Sigma||F_o| - |F_c||\Sigma|F_o|$ for $F_o > 2\sigma(F_o)$; $wR2 = (\Sigma w(F_o^2 - F_c^2)^2/\Sigma(wF_c^2)^2)^{1/2}$ all reflections; $w = 1/[\sigma^2(F_o^2) + (0.121P)^2 + 0.825P]$ where $P = (F_o^2 + 2F_c^2)/3$.